Supporting Information

Sc Dopant Induced Tailoring of Persistent Luminescence in $Na_3YSi_3O_9:Eu^{2+}$ For Information Recording

Kang Zhang[1], Bo Wang[1*], Tianpeng Liu[1], Hongxiang An[1], Shuwei Deng[1], Zhiyu Hu[1], Youchao Kong[2*], and Qingguang Zeng[1*]

[1]School of Applied Physics and Materials, Wuyi University, Jiangmen, Guangdong 529020, P.R. China

[2]Department of Physics and Electronic Engineering, Yancheng Teachers University, Yancheng 224002, China

Corresponding Authors:

Bo Wang: wangbo312@mails.ucas.ac.cn

Youchao Kong: yb87816@connect.um.edu.mo;

Qingguang Zeng: zengqg@mail.ustc.edu.cn

2. Experimental section:

2.1 Sample preparation

All phosphors were synthesized using a traditional solid-state method. The raw materials were Na_2CO_3 (99.99%), Y_2O_3 (A.R.), Sc_2O_3 (99.99%), SiO_2 (A.R.), and Eu_2O_3 (99.99%), which were used directly without any further treatment. The stoichiometric starting materials were thoroughly homogenized, the mixture was transferred into an alumina crucible and then loaded into a muffle furnace. Then the mixed samples were sintered at 1250 ℃ for 5 h under 95% N_2+5% H_2 reductive atmosphere. The obtained samples were cooled to room temperature and then ground again in an agate mortar.

2.2 Characterization

The powder X-ray diffraction (PXRD) patterns of the as-obtained samples were collected on a X' Pert PRO diffractometer (Cu Kα radiation, λ = 1.5406 Å) at 298 K. The microstructure was analyzed using a scanning electron microscope (SEM, JSM-6700F) and transmission electron microscope (FE-TEM, JEM-2100F, JEOL). The X-ray photoelectron spectroscopy (XPS, Thermo fisher Scientific K-Alpha) was conducted to identify the chemical states of the elements in the sample. A FLS-980 fluorescence spectrophotometer (Xe 900, 450 W arc lamps) was employed to obtain the photoluminescence (PL), photoluminescence excitation (PLE), and decay curve spectra. An absolute photoluminescence quantum yield measurement system (Hamamatsu, Quantaurus-QY plus C13534-31) was adopted to test the quantum efficiency. A LTTL-3DS measurement was used to record the 3D TL glow curves at a

heating rate of 1 K•s^{-1}.

2.3 Computational methods:

Utilizing density functional theory (DFT) as implemented in the Vienna *ab-initio* simulation package code,[1] we investigate the electronic structures of title compound. We used projector augmented wave (PAW) method[2] for the ionic cores and the generalized gradient approximation (GGA) for the exchange-correlation potential, in which the Perdew-Burke-Ernzerhof (PBE) type[3] exchange-correlation was adopted. The reciprocal space was sampled with 0.03 Å^{-1} spacing in the Monkhorst-Pack scheme for structure optimization, while denser k-point grids with 0.01 Å^{-1} spacing were adopted for properties calculation. We used a mesh cutoff energy of 400 eV to determine the self-consistent charge density. All geometries are relaxed until the Hellmann-Feynman force on atoms is less than 0.01 eV/Å and the total energy change is less than 1.0×10^{-5} eV. The calculation models were built from the crystal structure.

[1] A. G. Kresse, J. Furthmüller, Efficient iterative schemes for ab initio total-energy calculations using a plane-wave basis set. Phys. Rev. B 1996, 54, 11169.

[2] B. G. Kresse, J. Furthmüller, Efficiency of Ab-initio total energy calculations for metals and semiconductors using a plane-wave basis set. Com. Mater. Sci. 1996, 6, 15-50.

[3] J. P. Perdew, K. Burke, M. Ernzerhof, Generalized gradient approximation made simple. Phys. Rev. Lett. 1996, 77, 3865.

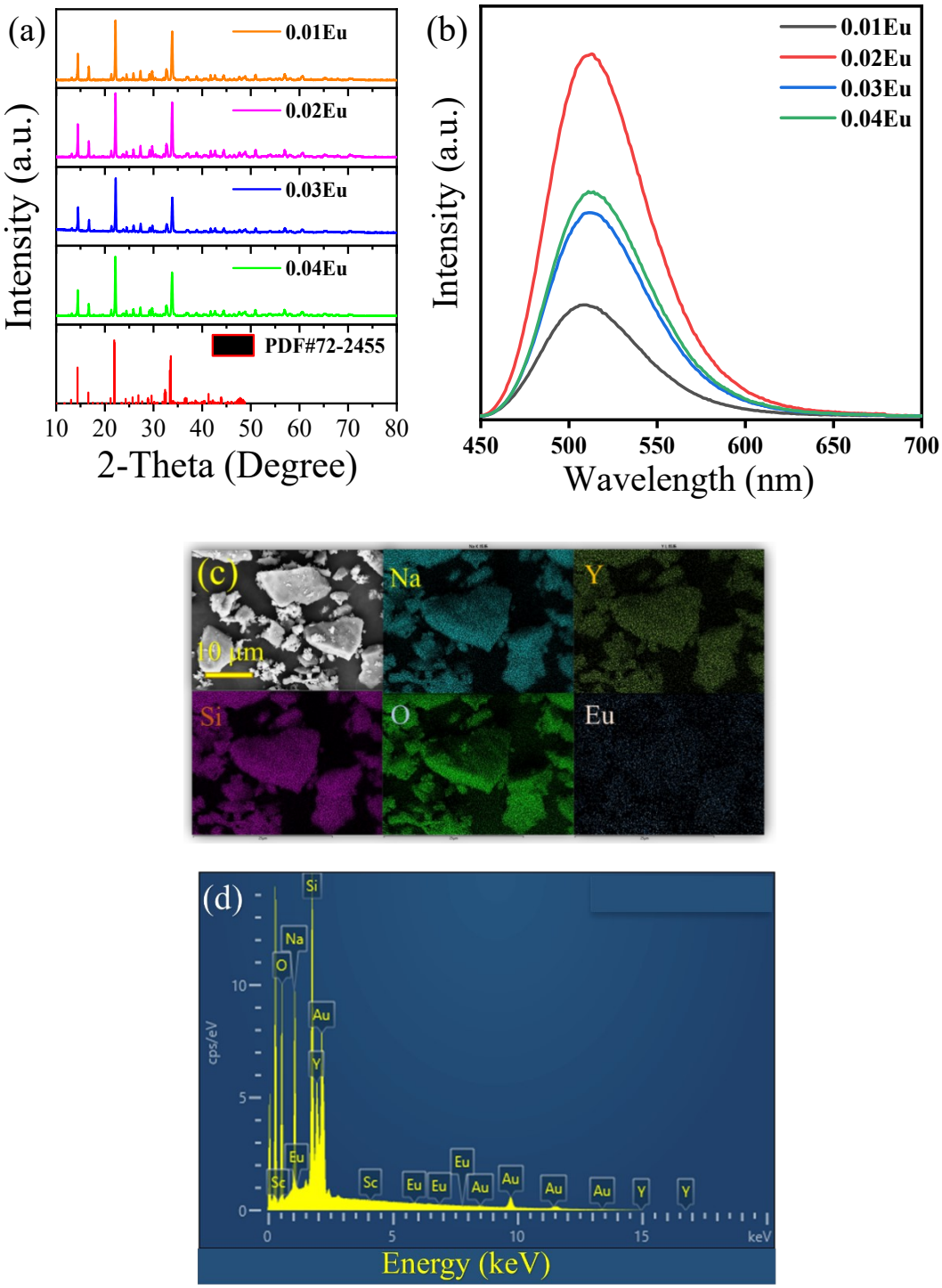

Figure S1. (a) The XRD patterns of $Na_3YSi_3O_9$:xEu^{2+} (x = 0.01, 0.02, 0.03 and 0.04). (b) The PL spectra of $Na_3YSi_3O_9$:xEu^{2+} (x = 0.01, 0.02, 0.03 and 0.04) samples. (c) (d) SEM image and EDS of $Na_3YSi_3O_9$:0.02Eu^{2+} microcrystal particles and elemental mapping images of Na, Y, Si, O, and Eu.

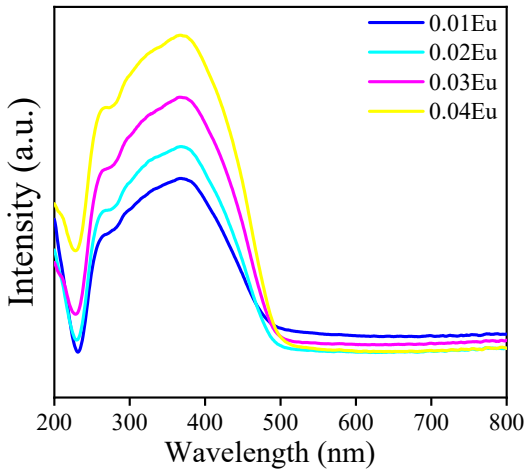

Figure S2. The UV-Vis spectra of $Na_3YSi_3O_9$:xEu^{2+} sample.

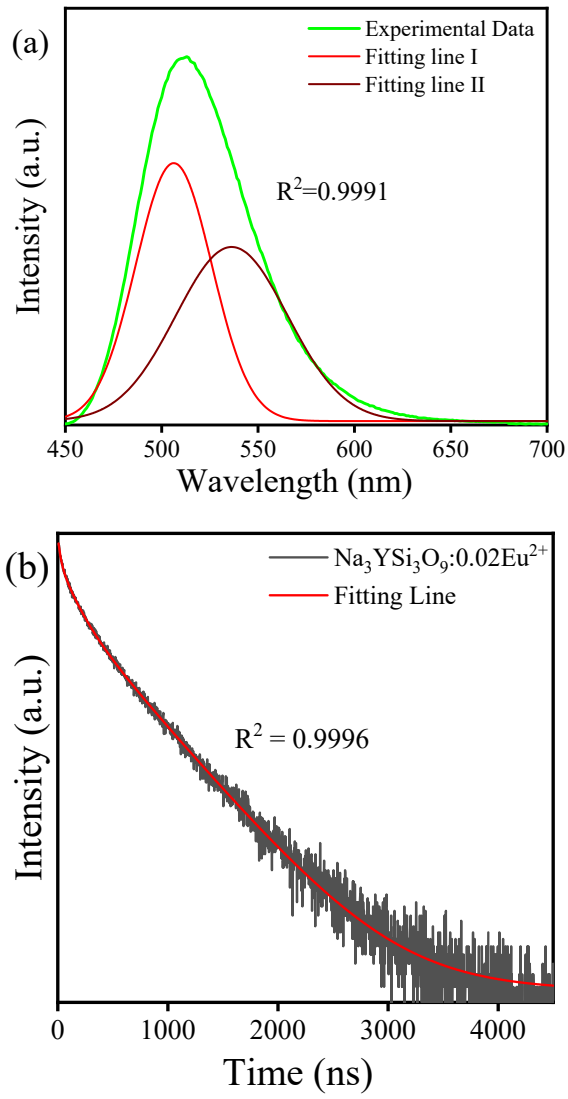

Figure S3(a). PL spectra and the PL deconvolution of $Na_3YSi_3O_9$:0.02Eu^{2+}. (b) Decay curve and fitting line of $Na_3YSi_3O_9$:0.02Eu^{2+}.

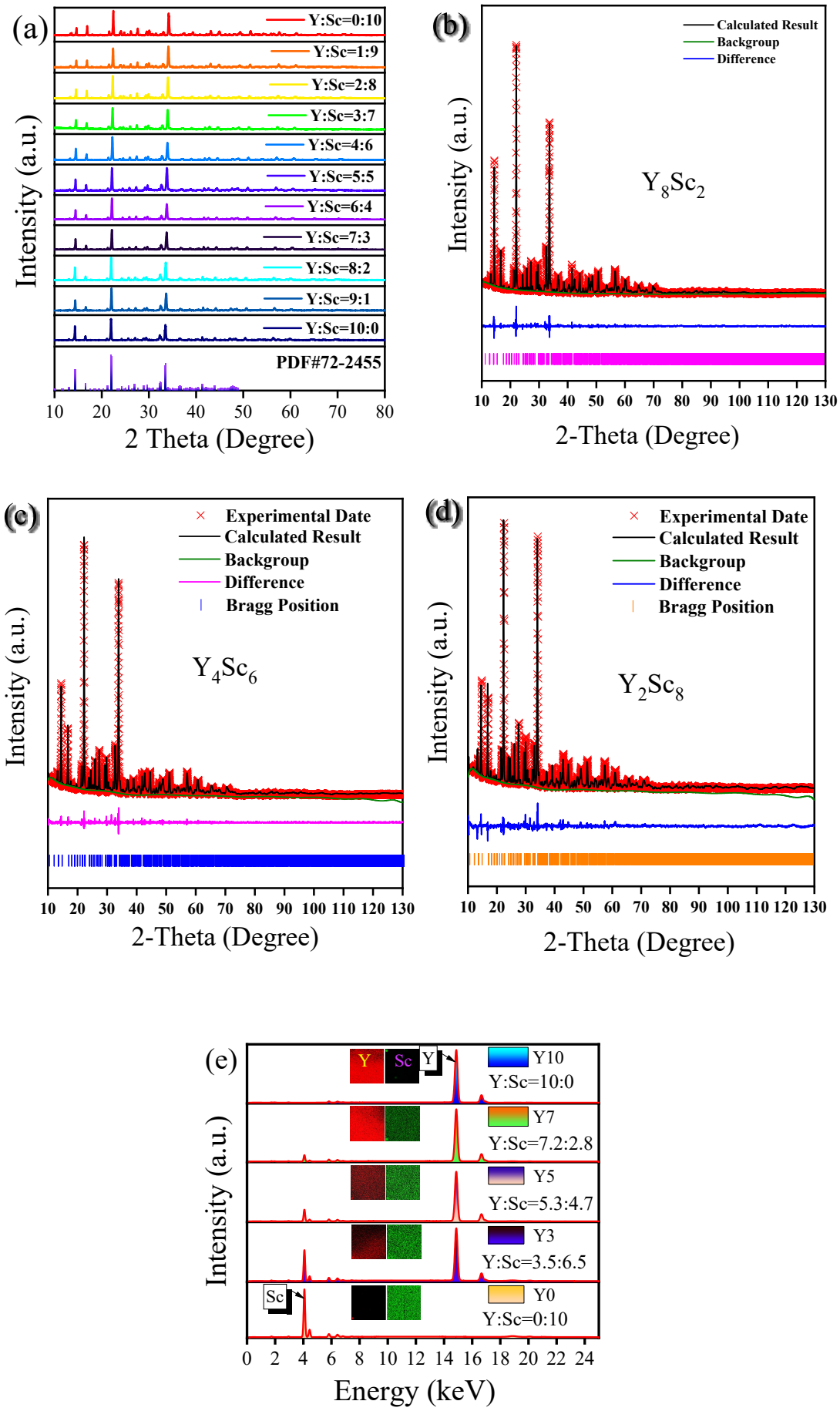
(a)
Y:Sc=0:10
Y:Sc=1:9
Y:Sc=2:8
Y:Sc=3:7
Y:Sc=4:6
Y:Sc=5:5
Y:Sc=6:4
Y:Sc=7:3
Y:Sc=8:2
Y:Sc=9:1
Y:Sc=10:0
PDF#72-2455
Intensity (a.u.)
2 Theta (Degree)
(b)
Calculated Result
Backgroup
Difference
Y_8Sc_2
Intensity (a.u.)
2-Theta (Degree)
(c)
Experimental Date
Calculated Result
Backgroup
Difference
Bragg Position
Y_4Sc_6
Intensity (a.u.)
2-Theta (Degree)
(d)
Experimental Date
Calculated Result
Backgroup
Difference
Bragg Position
Y_2Sc_8
Intensity (a.u.)
2-Theta (Degree)
(e)
Y
Sc
Y
Y10
Y:Sc=10:0
Y7
Y:Sc=7.2:2.8
Y5
Y:Sc=5.3:4.7
Y3
Y:Sc=3.5:6.5
Sc
Y0
Y:Sc=0:10
Intensity (a.u.)
Energy (keV)

Figure S4. (a) The XRD patterns of $Na_3Y_{1-y}Sc_ySi_3O_9$:0.02Eu^{2+} samples. (b-d) Observed and calculated XRD patterns of $Na_3Y_{0.8}Sc_{0.2}Si_3O_9$:$Eu^{2+}$, $Na_3Y_{0.4}Sc_{0.6}Si_3O_9$:$Eu^{2+}$ and $Na_3Y_{0.2}Sc_{0.8}Si_3O_9$:$Eu^{2+}$ (e) The EDS spectra of $Na_3Y_{1-y}Sc_ySi_3O_9$:0.02Eu^{2+} samples by conducting XRF.

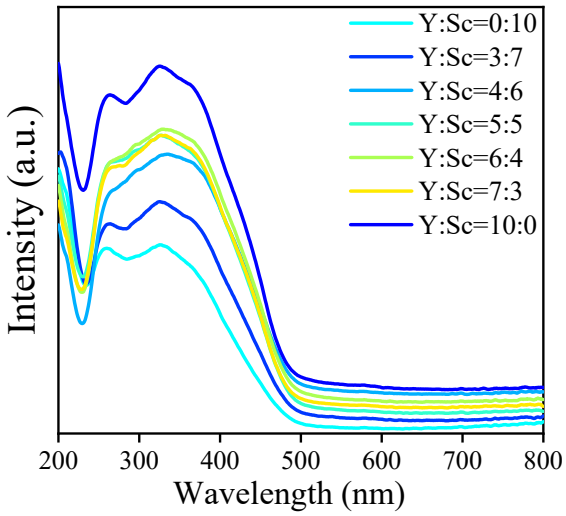

Figure S5. The UV-Vis absorption spectra of $Na_3(Y,Sc)Si_3O_9:Eu^{2+}$ samples.

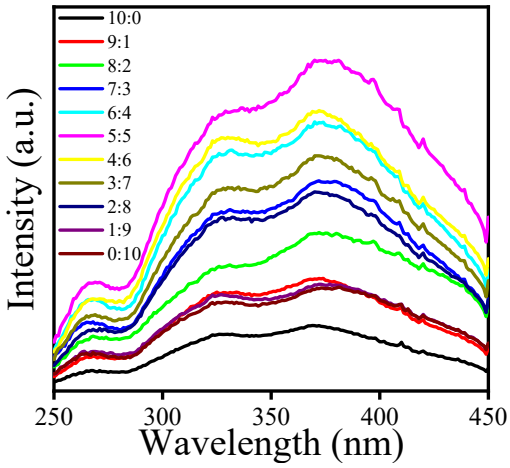

Figure S6. The PLE spectra of $Na_3(Y_ySc_{1-y})Si_3O_9:Eu^{2+}$ phosphors with y = 0-1.

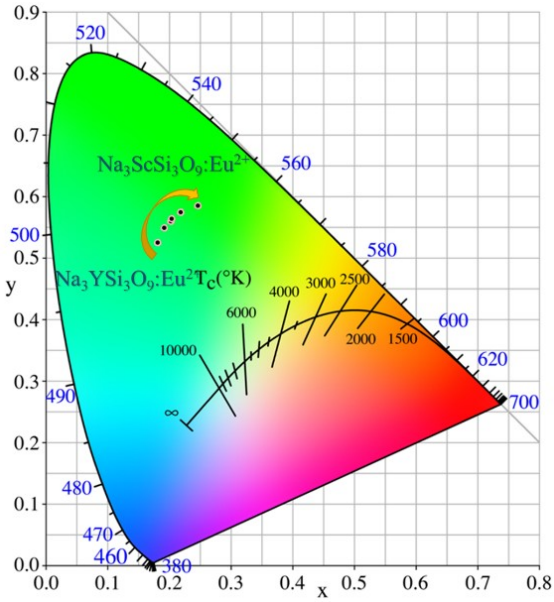

Figure S7. The CIE chromaticity coordinates diagram for $Na_3(Y,Sc)Si_3O_9:Eu^{2+}$.

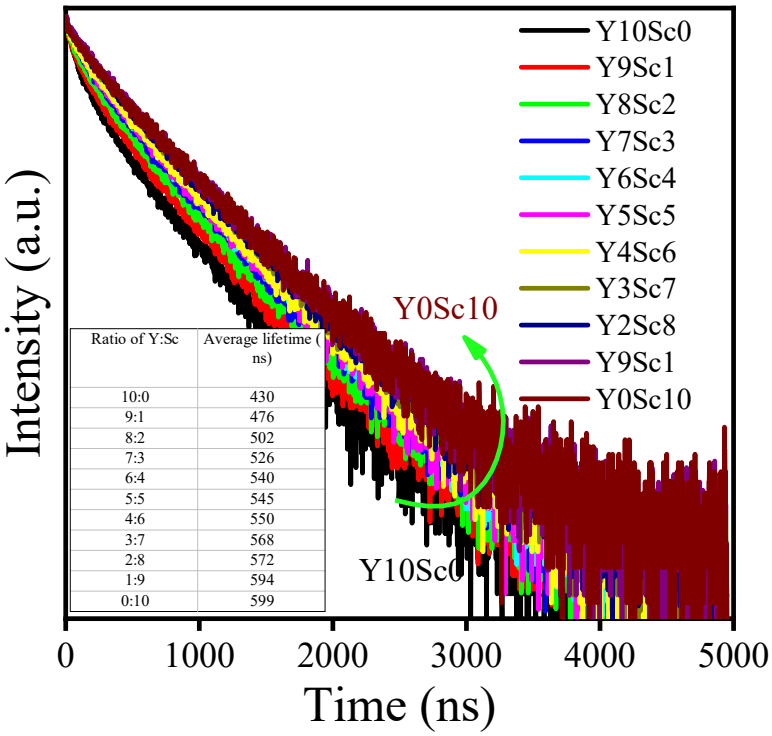

Ratio of Y:Sc	Average lifetime (ns)
10:0	430
9:1	476
8:2	502
7:3	526
6:4	540
5:5	545
4:6	550
3:7	568
2:8	572
1:9	594
0:10	599

Figure S8. The decay curves of $Na_3Y_{1-y}Sc_ySi_3O_9$:0.02Eu^{2+} samples.

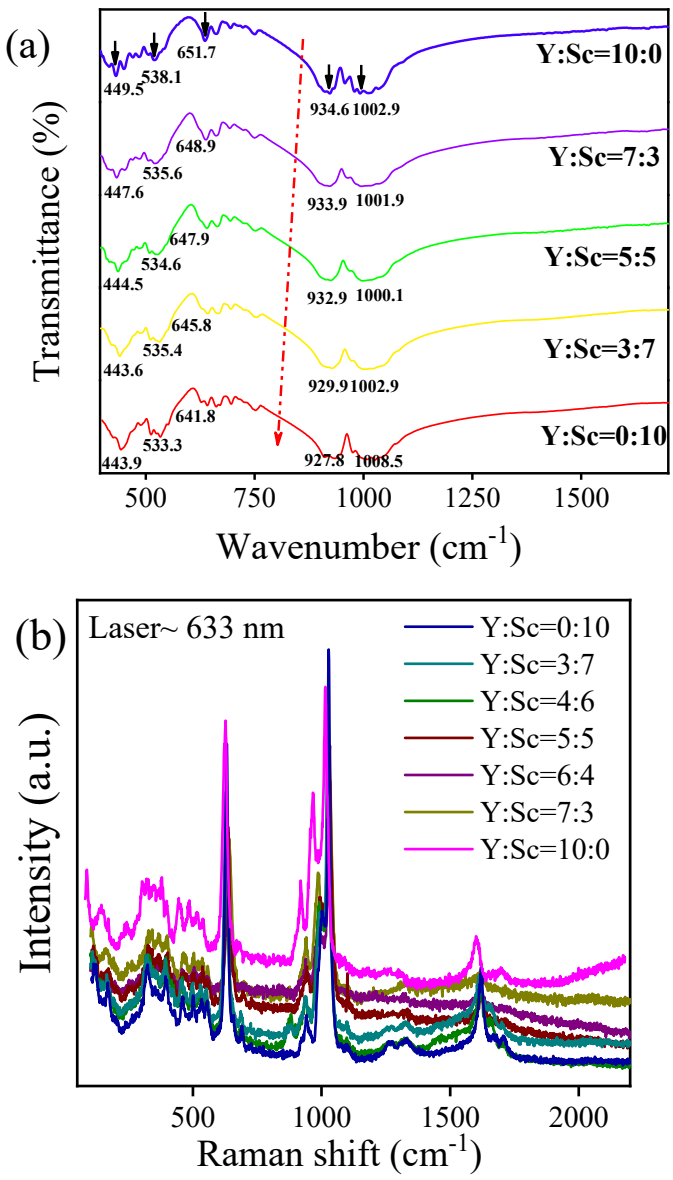

Figure S9(a)(b). The FTIR and Raman spectra of $Na_3Y_{1-y}Sc_ySi_3O_9$:0.02Eu^{2+} (y = 0-1) samples.

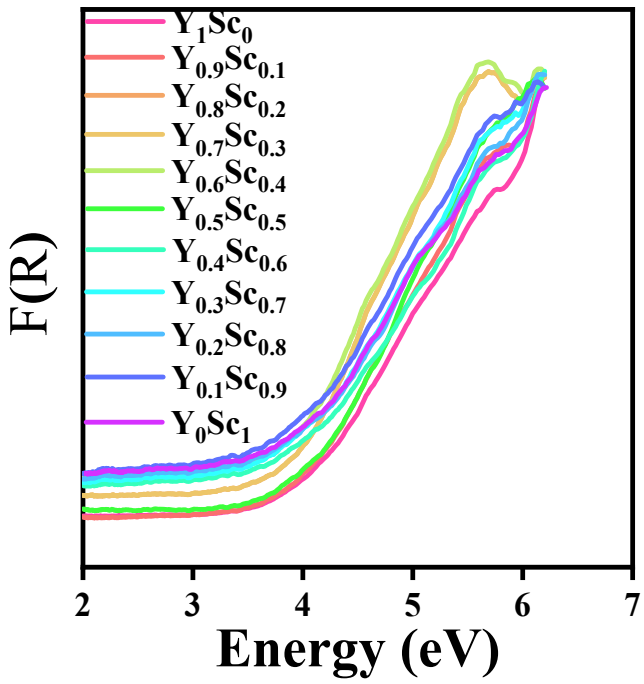

Figure S10. Normalized absorption spectra of $Na_3Y_{1-y}Sc_ySi_3O_9$ (y = 0-1) host.

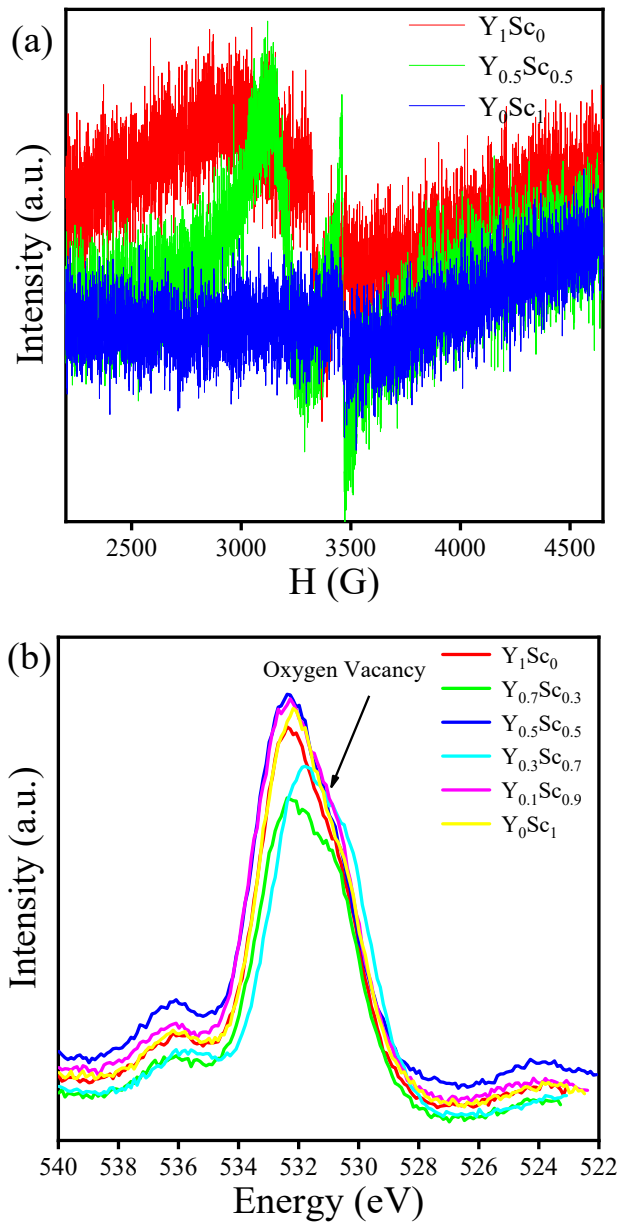

Figure S11. (a) The EPR spectra of $Na_3YSi_3O_9:Eu^{2+}$, $Na_3Y_{0.5}Sc_{0.5}Si_3O_9:Eu^{2+}$ and $Na_3ScSi_3O_9:Eu^{2+}$ phosphors. (b) The O-XPS spectra of $Na_3(Y_{1-y}Sc_y)Si_3O_9:Eu^{2+}$ (y = 0, 0.3, 0.5, 0.7, 1) phosphors.

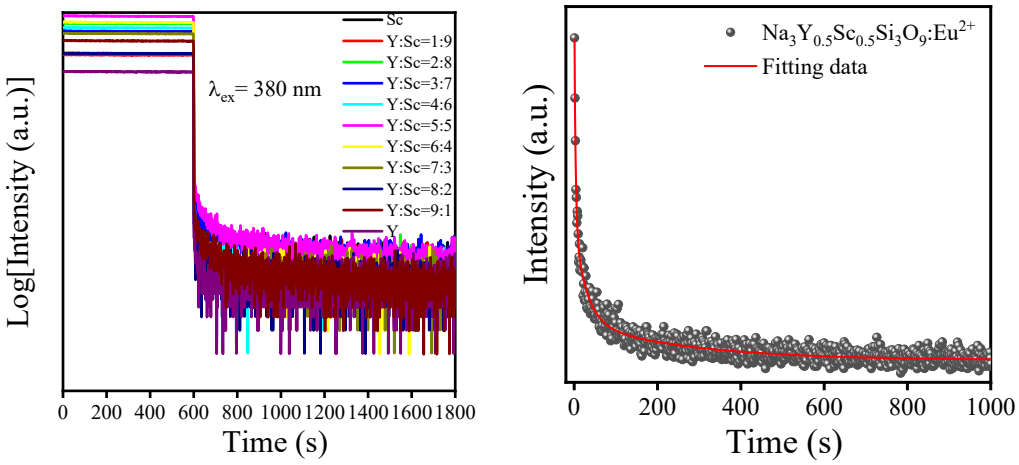

Figure S12. The long afterglow decay curves of $Na_3(Y_{1-y}Sc_y)Si_3O_9:Eu^{2+}$ (y = 0-1) phosphors.

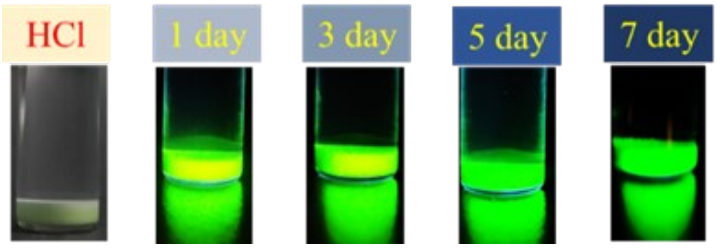

Figure S13. PL brightness images of $N_3Y_{0.5}Sc_{0.5}Si_3O_9:Eu^{2+}$ under HCl solutions.

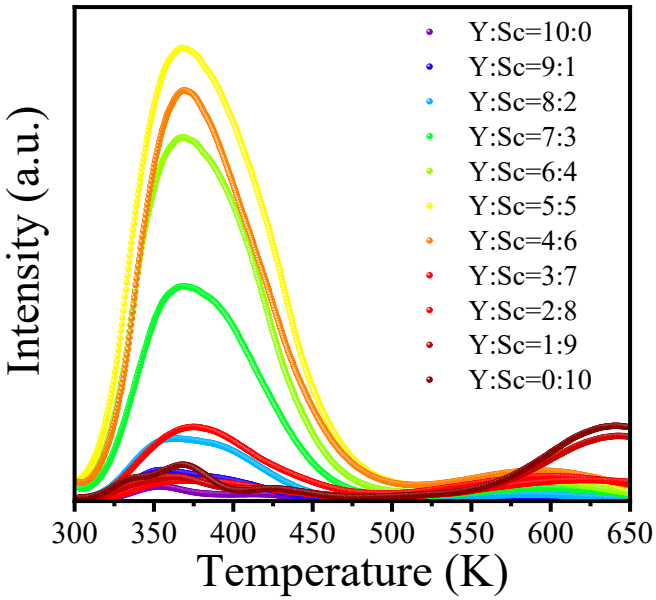

Figure S14. The 2D TL spectra of $Na_3(Y_{1-y}Sc_y)Si_3O_9:Eu^{2+}$ (y = 0-1) phosphors.

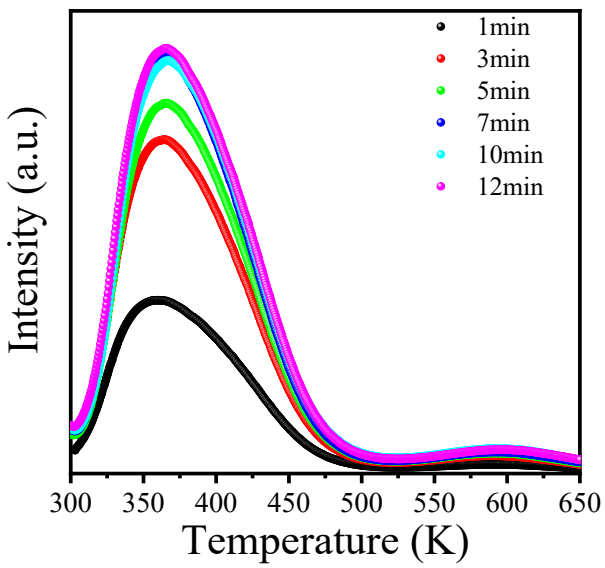

Figure S15. Excitation duration dependent TL glow curves at a heating rate of 1K/s.

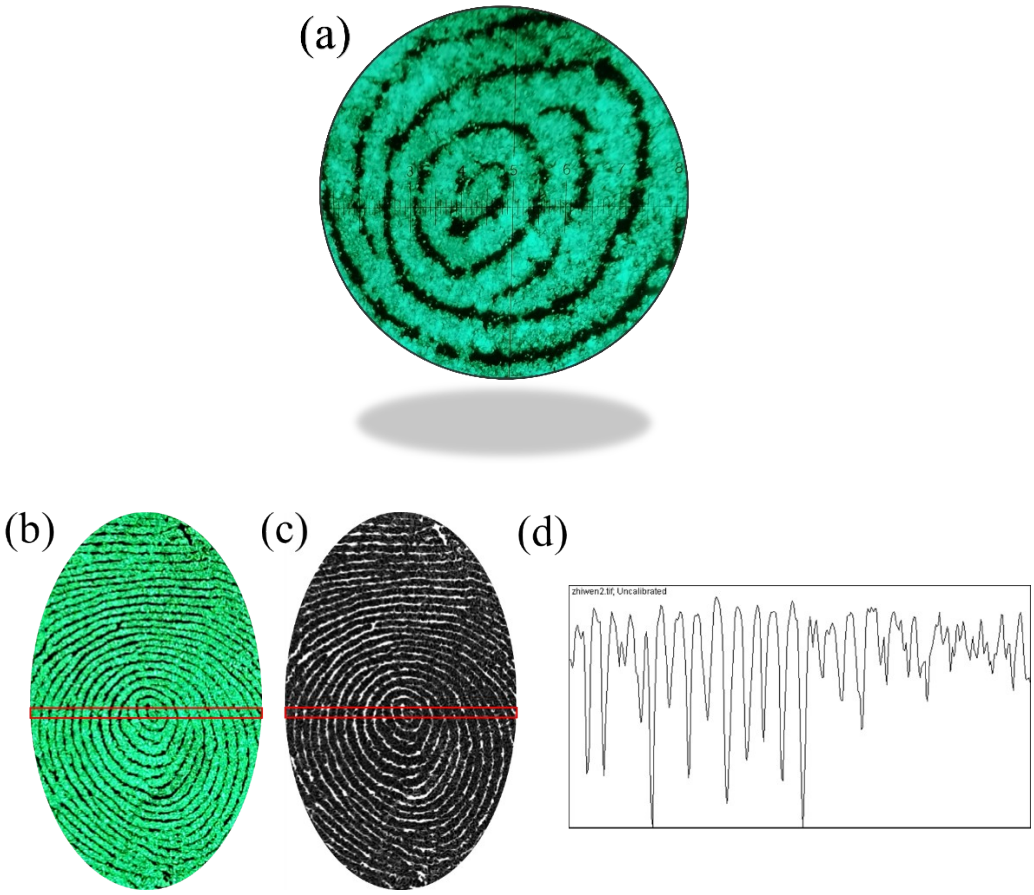

Figure S16. (a) The magnified image of core show specific detail. (b) The digital photograph. (c) the grayscale photos. (d) the gray value over the LFPs.

Table S1. Fractional atomic coordinates, bond lengths (Å) and coordination number.

Atom	x	y	z	Average Na-O (Å)	Coordination Number
Na1	0.1509	0.3694	0.3881	2.45	5
Na2	0.1190	0.1680	0.6301	2.31	8
Na3	0.3935	0.0936	0.6363	2.50	5
Na4	0.4438	0.4468	0.9972	2.19	3
Na5	0.1619	0.1227	0.8977	2.49	7
Na6	0.1205	0.4014	0.8488	2.42	6
Na7	0.1524	0.1242	0.3537	2.46	5
Na8	0.0036	0.009	0.4963	2.36	4
Na9	0.0978	0.3449	0.1278	2.37	5
Na10	0.2944	0.2467	0.2020	2.48	4
Na11	0.4119	0.1261	0.3828	2.68	5
Na12	0.2889	0.2913	0.7493	2.61	6

Table S2. The Rietveld refinement and average bond length of Na-O.

Ratio of Y:Sc	R_p(%)	R_{wp}(%)	R_{exp}(%)	χ^2
10:00	9.5	10.3	6.8	1.51
8:2	12.3	11.9	8.9	1.48
5:5	10.4	12.8	7.7	1.66
4:6	13.9	13.2	8.6	1.53
2:8	11.7	10.6	7.9	1.34
0:10	13.2	14.1	8.3	1.71

Ratio of Y:Sc	Average band length of Na8-O (Å)	Average band length of Na7-O (Å)
10:0	2.31	2.49
8: 2	2.29	2.45
6:4	2.25	2.41
5:5	2.23	2.39
4:6	2.19	2.36
2:8	2.15	2.31
0:10	2.11	2.95

Table S3. The afterglow decay times (τ) of $Na_3(Y,Sc)Si_3O_9:Eu^{2+}$.

Sample	τ_1	τ_2	τ_3
Y:Sc=10:0	1.9	10.1	128.3
Y:Sc=9:1	1.4	15.9	137.2
Y:Sc=8:2	1.8	24.4	259.7
Y:Sc=7:3	3.1	29.4	323.4
Y:Sc=6:4	3.4	34.3	446.1
Y:Sc=5:5	4.2	60.8	531.0
Y:Sc=4:6	3.4	33.3	411.4
Y:Sc=3:7	2.6	30.9	407.1
Y:Sc=2:8	2.2	28.4	290.1
Y:Sc=1:9	2.1	21.1	226.6
Y:Sc=0:10	1.9	18.4	150.7